POSTBUCKLING RESPONSE OF GRAPHITE-EPOXY PLATES LOADED IN COMPRESSION

Flat unstiffened rectangular plates were loaded to failure in compression to study their postbuckling behavior (ref. 1). Unidirectional tapes of Thornel 300 graphite fibers preimpregnated with Narmco 5208 epoxy resin (T300/5208) were used to make 16- and 24-ply quasi-isotropic and 24-ply $[\pm 45/0_2/\pm 45/0_2/\pm 45/0/90]_s$ orthotropic plates. The plates were 20 inches long and from 3.5 to 9.0 inches wide. The loaded ends of the plates were clamped and the sides were simply supported.

Load-shortening results from the tests are summarized below in Figure 1. The applied load P is normalized by the buckling load P_{cr} and the measured end shortening u is normalized by the end shortening at buckling u_{cr}. Buckling is indicated by the filled circle and failure is indicated by the open symbols. All specimens had some postbuckling response. Specimens with lower values of width-to-thickness ratio (e.g, b/t = 24) failed at applied loads that are slightly higher than the buckling load. Specimens with higher values of width-to-thickness ratio (e.g., b/t = 115) failed at applied loads that are several times larger than the buckling load.

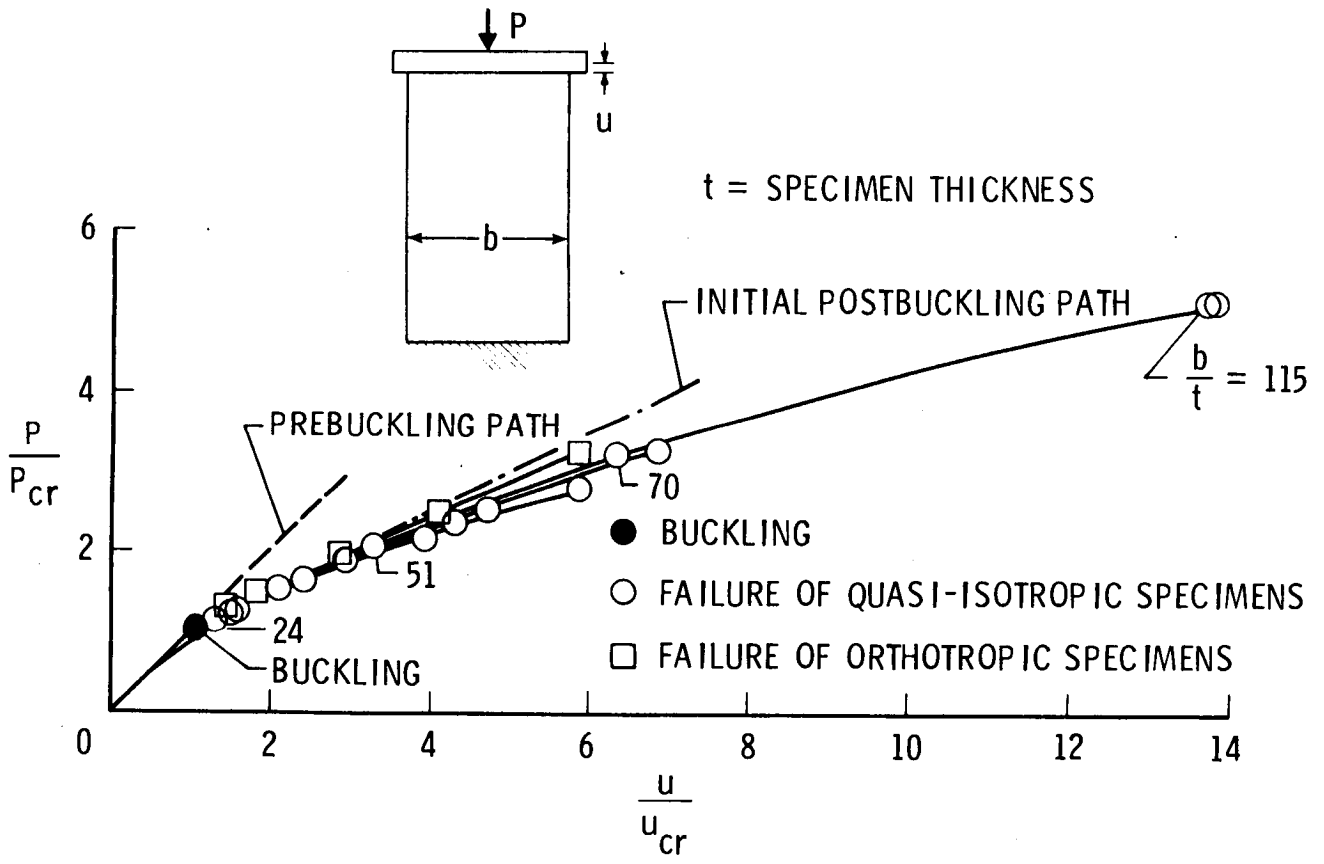

Figure 1

STRAIN DISTRIBUTION AND FAILURE MODE OF A GRAPHITE-EPOXY PLATE

Longitudinal strain distributions across the width of a typical buckled specimen in Figure 1 are shown below in Figure 2 for an applied compressive load of about three times the buckling load. The figures on the left of Figure 2 show typical measured surface strain data from back-to-back strain gages and the resulting computed membrane strains across a nodal line of the buckling mode and across the plate at a point of maximum buckling mode amplitude. These data show that the membrane strains are low in the interior of the buckled plate and high at the edges of the plate.

The buckling mode shape of the typical specimen is represented by the moire-fringe pattern shown in the left photograph. The panel failed along a nodal line of the buckling mode as indicated by the moire-fringe pattern shown in the center photograph. Apparently, the higher membrane strains near the specimen edges couple with the out-of-plane deflection gradients at the nodal line to cause the shear failure shown in the right photograph.

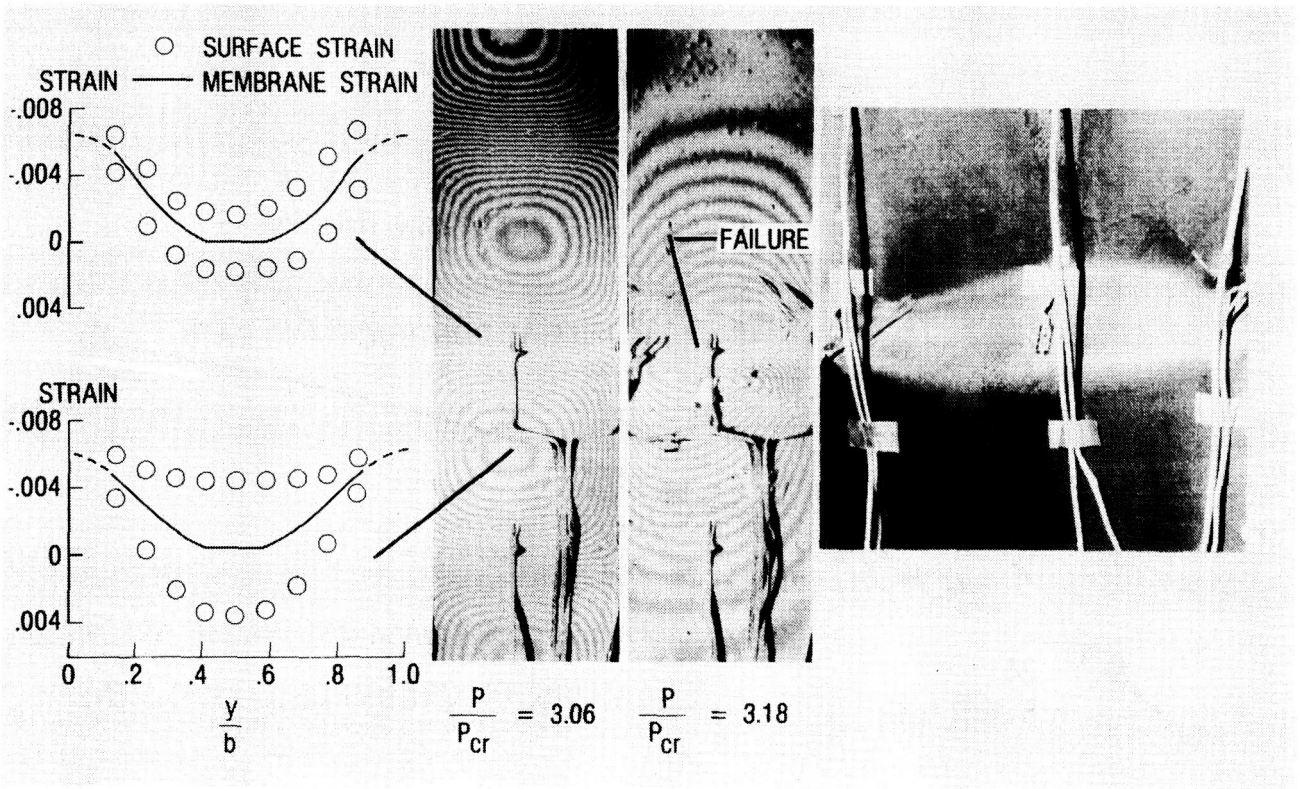

Figure 2

POSTBUCKLING RESPONSE OF FLAT GRAPHITE-EPOXY PLATES WITH HOLES

The effects of circular holes on the postbuckling behavior of flat T300/5208 graphite-epoxy plates similar to those described in Figure 1 were studied in reference 1 and some typical results are shown in Figure 3. Back-to-back strain gages were distributed across the specimen along a lateral line (labeled Y on the lower right figure) that passes through the center of the hole. For applied loads P less than the buckling load P_{cr} these strain gages indicate that a membrane strain gradient exists near the hole as shown in the upper left figure. The left photograph shows a moire-fringe pattern of the specimen before buckling and indicates that no out-of-plane deformations have occurred. The right photograph shows a moire-fringe pattern of the buckling mode shape with four longitudinal waves. For applied loads greater than the buckling load, the back-to-back strain gages indicate that the buckling mode shape has caused a severe local bending strain gradient to occur near the hole as shown in the upper right figure.

Measured end shortening results U for typical specimens with various hole diameters D and plates aspect ratios L/b equal to 2.2 and 5.0 are shown in the lower left figure as a function of the applied load P. End shortening is normalized by the plate length L and the applied load is normalized by the plate longitudinal modulus E and cross-sectional area A. The filled circles represent failure of specimens without holes and the open circles represent failure of specimens with holes. The results indicate that a hole had little effect on the postbuckling strength of the low-aspect-ratio specimens but the postbuckling strength of the high-aspect-ratio specimens decreased as the hole diameter increased.

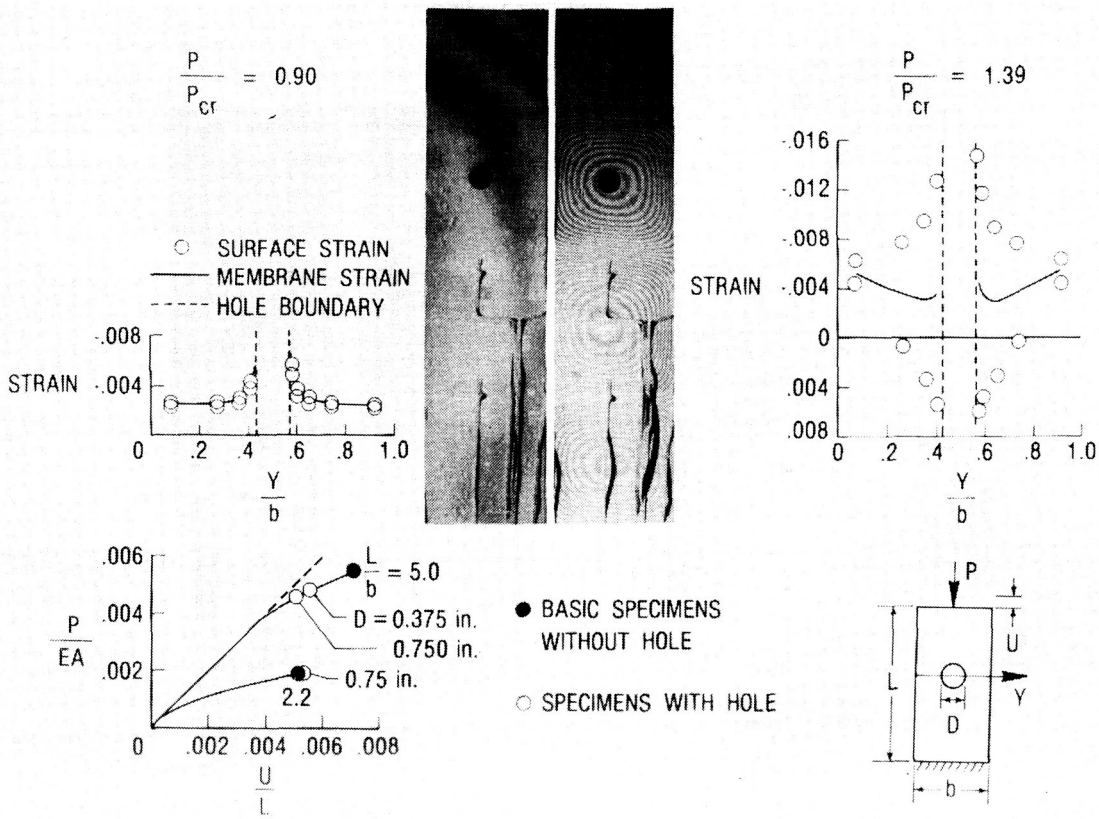

Figure 3

POSTBUCKLING RESPONSE OF FLAT GRAPHITE-EPOXY PLATES WITH LOW-SPEED IMPACT DAMAGE

The effects of low-speed impact damage on the postbuckling behavior of flat T300/5208 graphite-epoxy plates similar to those described in Figure 1 were studied in reference 1 and some typical results are shown below in Figure 4. Specimens were impacted with 0.5-inch-diameter aluminum balls at various impact speeds V and then tested to failure. Measured end shortening results U for typical 16- and 24-ply quasi-isotropic specimens are shown in the lower left figure as a function of the applied load P. End shortening is normalized by the plate length L and the applied load is normalized by the plate longitudinal modulus E and cross-sectional area A. The filled circles represent failure of specimens without impact damage and the open symbols represent failure of specimens with impact damage. The open circles represent failure of specimens impacted in the center and the open squares represent failure of 16-ply specimens impacted near a specimen side. The results indicate that impact damage in the center of the 16-ply specimens had little effect on postbuckling strength regardless of the impact speed. The left photograph shows the moire-fringe pattern corresponding to the out-of-plane deformations of a 16-ply specimen loaded to approximately three times the buckling load and the right photograph shows the moire-fringe pattern corresponding to the failed specimen. Failure occurred along a buckling-mode nodal line away from the impact site. The membrane strain distribution across the specimen just before failure is indicated in the upper left figure. Apparently, the strain in the center of a 16-ply specimen is not high enough to cause the impact damage to propagate to fail the specimen. The results also indicate that impact damage in the center of the 24-ply specimens and at the sides of the 16-ply specimens decreases postbuckling strength as impact speed increases. Apparently, the strains at these impact sites are high enough to cause the impact damage to propagate to fail the specimens.

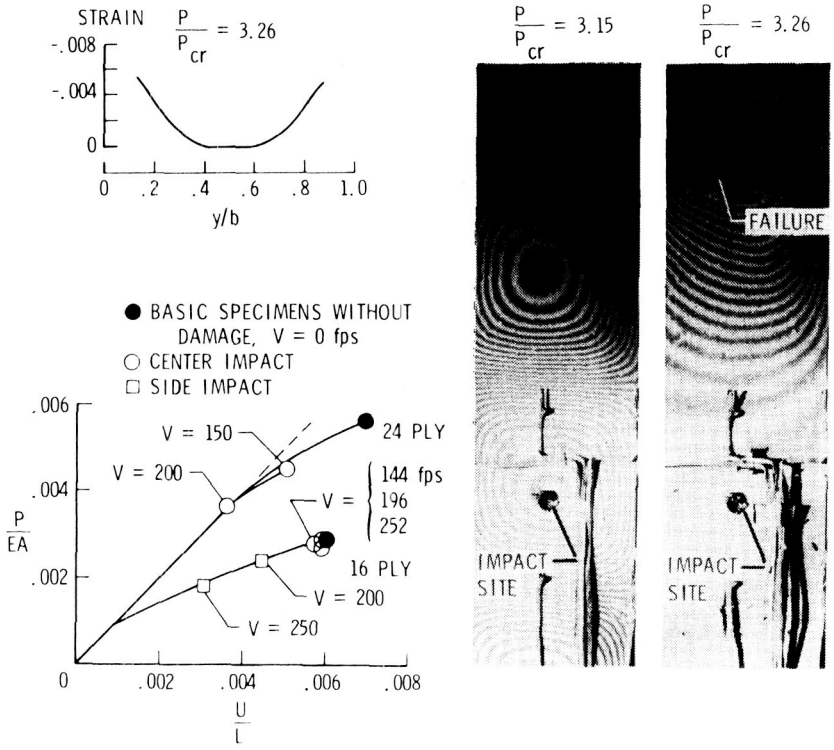

Figure 4

POSTBUCKLING RESPONSE OF FLAT GRAPHITE-EPOXY STIFFENED COMPRESSION PANELS

Flat graphite-epoxy stiffened panels were loaded to failure in compression to study their postbuckling behavior (ref. 2). The specimens were made from T300/5208 graphite-epoxy unidirectional tape and had four stiffeners of a common stiffener design. Specimens with 16- and 24-ply skins and 4.0-, 5.5- and 7.0-inch stiffener spacing were tested. A typical specimen is shown in the upper left photograph of Figure 5. Some typical results are also shown in Figure 5. Measured end shortening results u for specimens with various stiffener spacing b and skin thicknesses are shown in the upper figures as a function of the applied load P. End shortening is normalized by the panel length L and the applied load is normalized by the panel longitudinal modulus E and cross-sectional area A. All specimens exhibited some postbuckling capability. The open circles represent buckling and the crossed circles represent failure. The end loadings N_x at failure for the specimens ranged from 1400 lb/in to 4920 lb/in which is representative of transport fuselage loads. Back-to-back strain gages were distributed across the skin of the panels between the two interior stiffeners and some typical membrane strain results e are shown in the lower left figure for several values of applied load. The membrane strain is normalized by the strain at buckling e_{cr} and the applied load is normalized by the buckling load P_{cr}. The results indicate that the strains near the stiffeners are significantly higher than the strains in the center of the skin between stiffeners. All panels failed when the stiffeners separated from the skin as shown in the photograph and sketch at the lower right. Apparently, the high longitudinal strains at the stiffeners (shown in the lower left figure) interact with the out-of-plane deflection gradients at the stiffeners (shown in the lower center photograph of the moire-fringe pattern of out-of-plane displacements) to fail the panels.

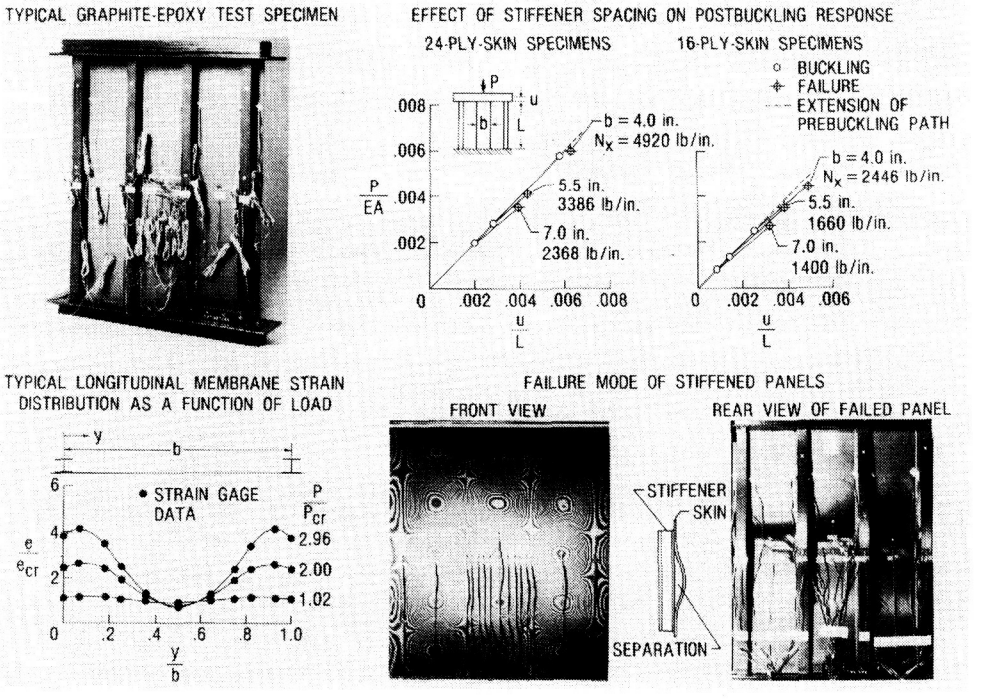

Figure 5

POSTBUCKLING ANALYSIS OF FLAT GRAPHITE-EPOXY
STIFFENED COMPRESSION PANEL

The STAGSC-1 nonlinear structural analysis code (ref. 3) was used in reference 2 to predict the response of a typical panel described in Figure 5 and the results are shown below in Figure 6. The results shown are for a panel with a 16-ply skin and 7.0-inch stiffener spacing. It was necessary to model the stiffener attachment flanges and webs with flexible plate elements in the finite element model used for the analysis in order to obtain the close agreement between test and analysis shown below. The contour plot at the upper left of the figure compares well with the photograph of the moire-fringe pattern of the out-of-plane deflections. The open circles in the figures below are test data and the solid lines are analytical data. The crossed circles represent failure of the specimens. The upper right figure compares results for end shortening u (normalized by end shortening at buckling u_{cr}) as a function of applied load P (normalized by the buckling load P_{cr}). The lower left figure compares results for measured out-of-plane deflection w at a point on the skin (normalized by the skin thickness t) as a function of applied load. The lower center figure compares strain results e from back-to-back strain gages on the skin (normalized by the strain at buckling e_{cr}) as a function of applied load. The lower right figure compares membrane strain distribution results across the panel skin between two stiffeners for several values of applied load. The results indicate that test and analysis compare well up to failure.

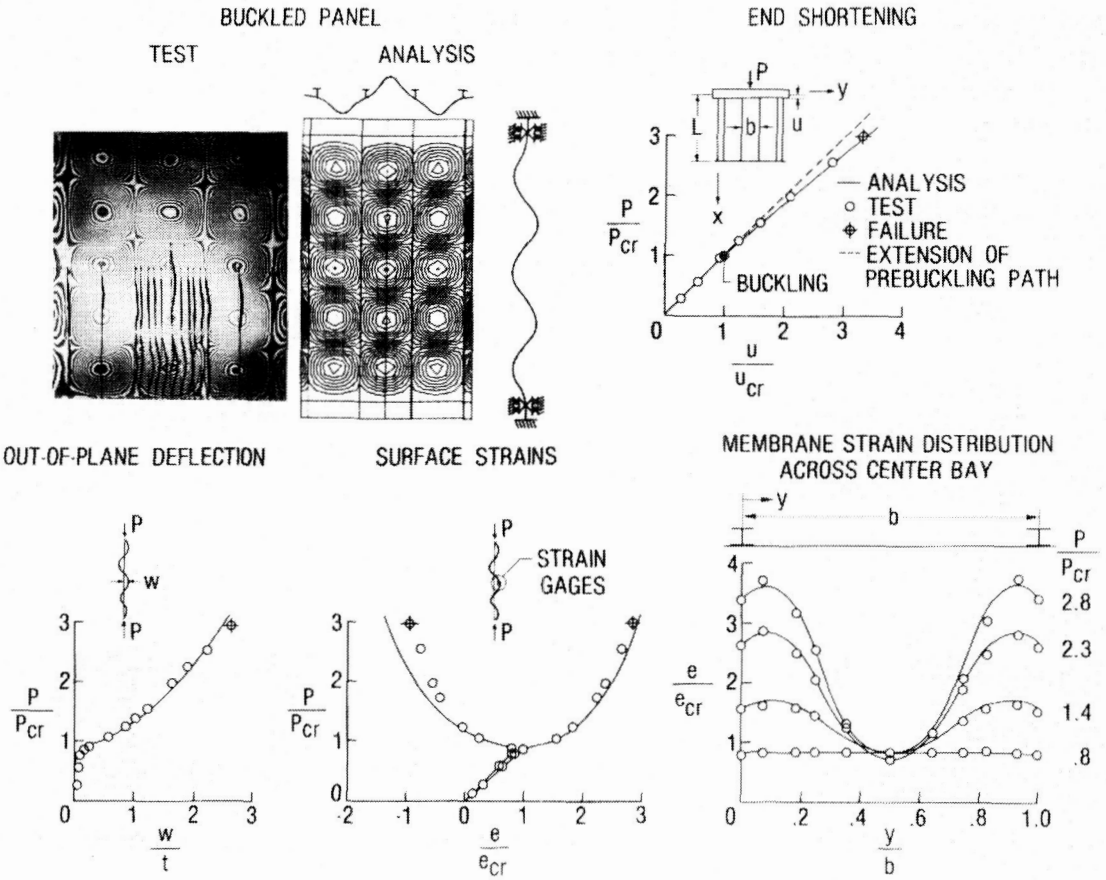

Figure 6

EFFECT OF CUT STIFFENERS ON POSTBUCKLING STRENGTH OF FLAT GRAPHITE-EPOXY COMPRESSION PANELS

Several T300/5208 graphite-epoxy stiffened panels, similar to those described in Figure 5, were subjected to low-speed impact damage and the results of residual strength tests on these damaged panels are presented in reference 2. It was found in reference 2 that low-speed impact damage could degrade the postbuckling strength of a panel if a region near a stiffener attachment flange were damaged. Several other stiffened panels, similar to those described in Figure 5, were damaged by cutting a 2.0-inch-long slot completely through the skin and one stiffener as indicated by the upper left figure in Figure 7. A slot was cut into panels with 16- and 24-ply skins and 4.0- and 7.0-inch stiffener spacing and then tested to failure to determine their residual strength. The results of these residual strength tests are shown below in Figure 7. End shortening results u (normalized by panel length L) are shown as a function of applied load P (normalized by panel longitudinal modulus E and cross-sectional area A). The results for undamaged specimens from Figure 5 are shown for comparison. The open circles represent panel buckling and the filled circles represent failure of the undamaged panels. The filled squares represent failure of the panels with slots. The results indicate that the slots degraded the postbuckling strength of the panels. The reduction in postbuckling strength observed for the slotted panels was greater than the reduction in postbuckling strength observed for the low-speed impact damaged panels reported in reference 2.

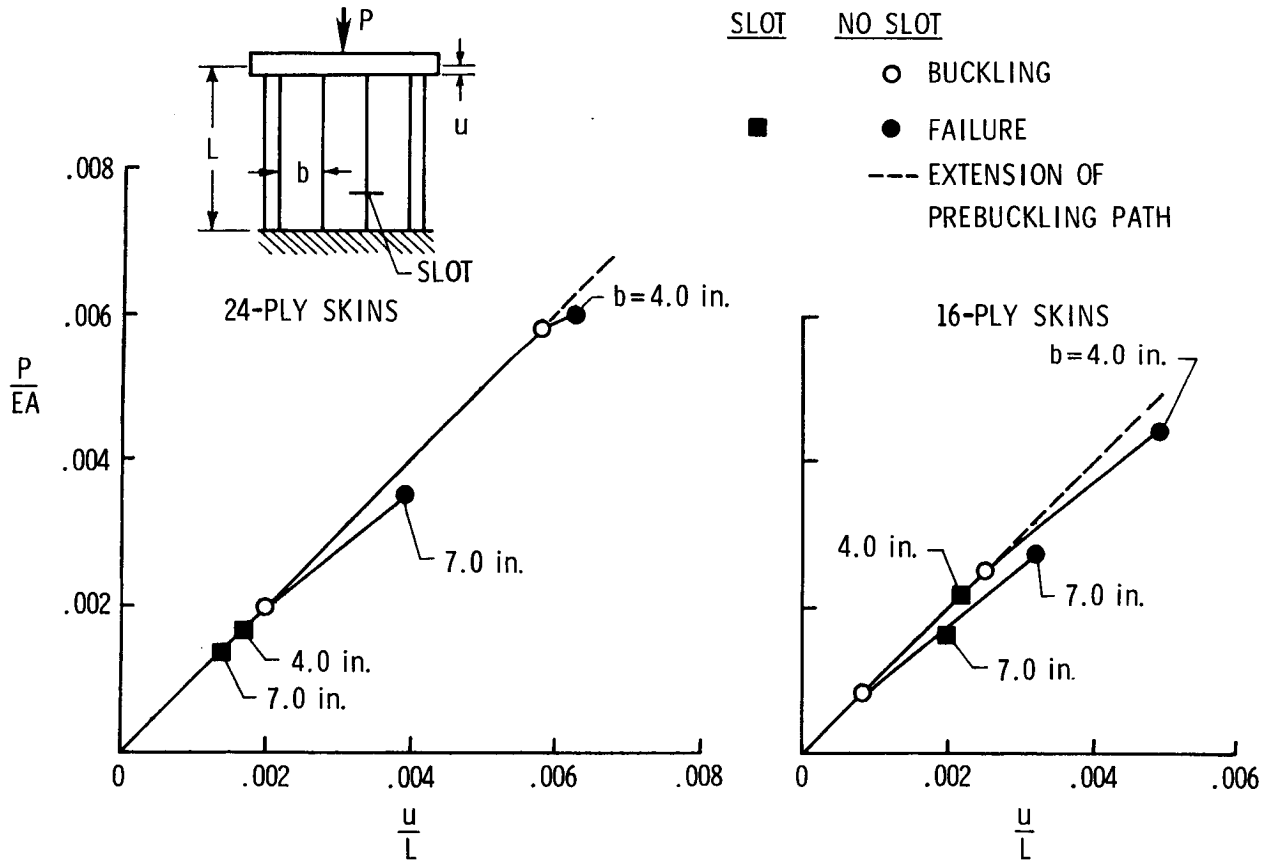

Figure 7

STIFFENER ATTACHMENT CONCEPTS FOR PANELS DESIGNED TO BUCKLE

Failure of the stiffened panels described in Figure 5 was caused by separation of the stiffener from the panel skin. Three stiffener attachment concepts that were intended to suppress the skin-stiffener separation failure mode have been evaluated to determine their effectiveness. Four Hercules AS4/3502 graphite-epoxy panels with 16-ply skins were made with a single stiffener attached to a skin with one of four stiffener attachment concepts. A typical specimen is shown in the upper left photograph in Figure 8. One specimen had the stiffener bonded to the skin with a secondary bonding operation to represent the stiffener attachment concept used for the panels described in Figure 5. The second specimen had a bonded stiffener reinforced with mechanical fasteners through the skin and stiffener attachment flanges. The attachment flanges of the third specimen were stitched to the skin and the skin and stiffener were cocured. The fourth specimen was based on the padded skin concept described in reference 4 and includes an additional twelve plies of AS4/3502 tape in the skin under the stiffener as shown in the lower left figure. The four panels were tested to failure and the results of the tests are shown in the lower right figure. The failure loads of the panels with mechanical fasteners and stitching were both higher than the failure load for the panel with the constant-thickness 16-ply skin and bonded stiffener. However, the failure load of the panel with the padded skin was higher than the failure loads of the other three panels. While the panel with the padded skin was approximately nine percent heavier than the panel with the bonded stiffener, its failure load was 30 percent higher. The panel with the padded skin failed by stiffener crippling as shown in the upper right photograph rather than by skin-stiffener separation.

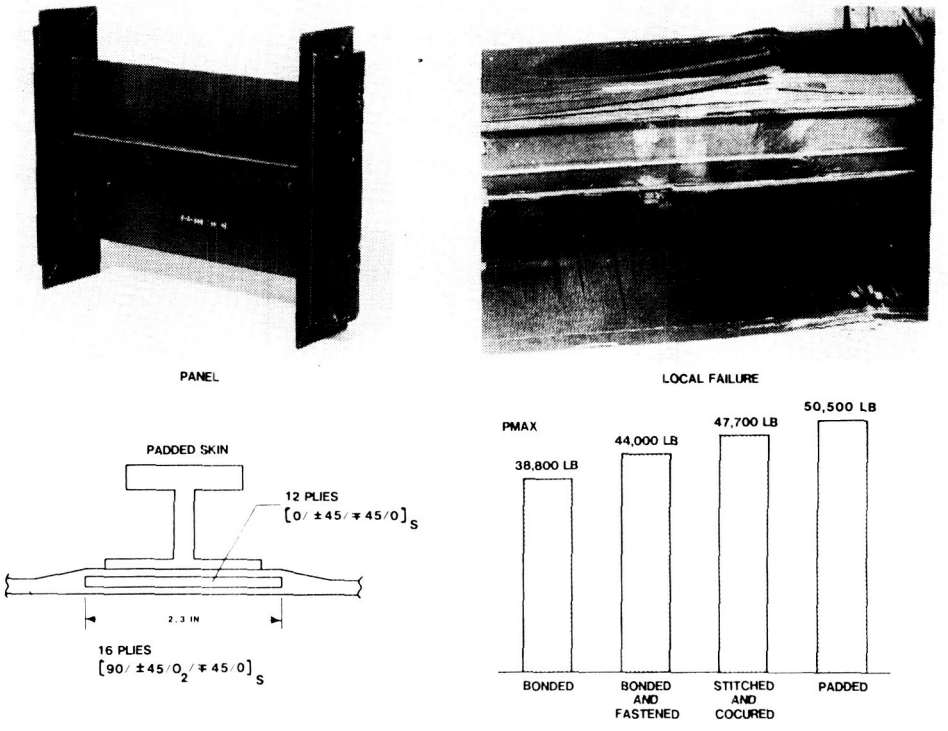

Figure 8

The effect of circular holes on the postbuckling response of curved T300/5208 graphite-epoxy panels is shown below in Figure 9. The results are for 16-ply quasi-isotropic panels with a 15 inch radius. The panels are 14 inches long and have a 14 inch arc length. Panels with no hole and with 0.5-, 1.0- and 2.0-inch-diameter holes were tested to failure. The panels were tested in a manner similar to that described for the panels in Figure 1. All panels exhibited some postbuckling capability. As shown in the figure, the panel with no hole (a = 0) and the panel with the 0.5-inch-diameter hole supported higher postbuckling loads than the panels with 1.0- and 2.0-inch-diameter holes. Severe local bending occurs near the hole after buckling as indicated in the photograph of the moire-fringe pattern of the buckling mode of the panel with the 1.0-inch-diameter hole. This severe local bending caused delamination to occur at the hole edge as shown in the photograph of the 2.0-inch-diameter hole edge shown in Figure 10. Apparently, the delamination at the hole edge reduced the local stiffness of the panel enough to reduce the postbuckling strength of the panels with the larger holes.

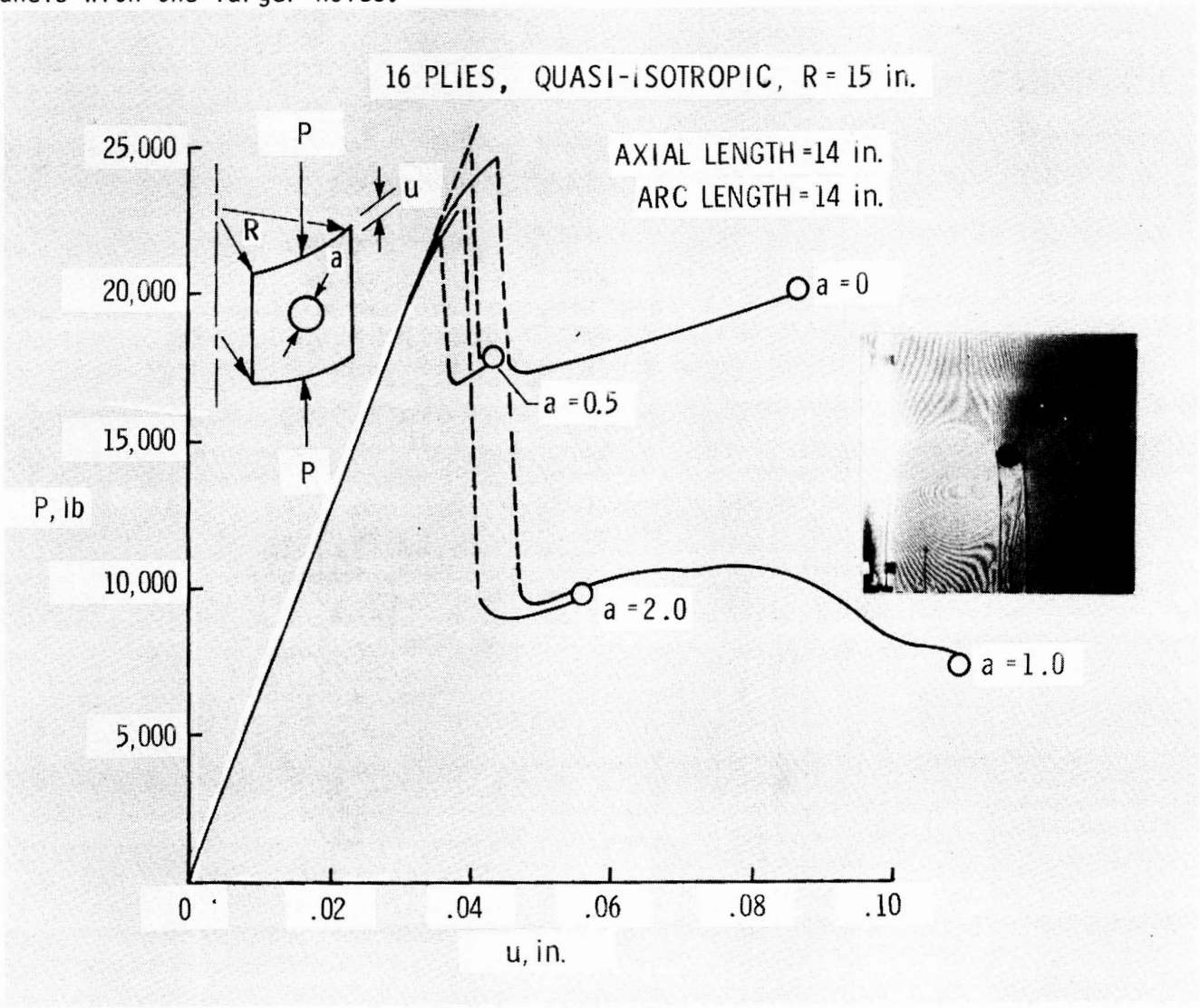

Figure 9

DELAMINATED HOLE EDGE OF CURVED GRAPHITE-EPOXY PANEL

The delaminated hole edge of the panel with the 2.0-inch-diameter hole described in Figure 9 is shown in Figure 10.

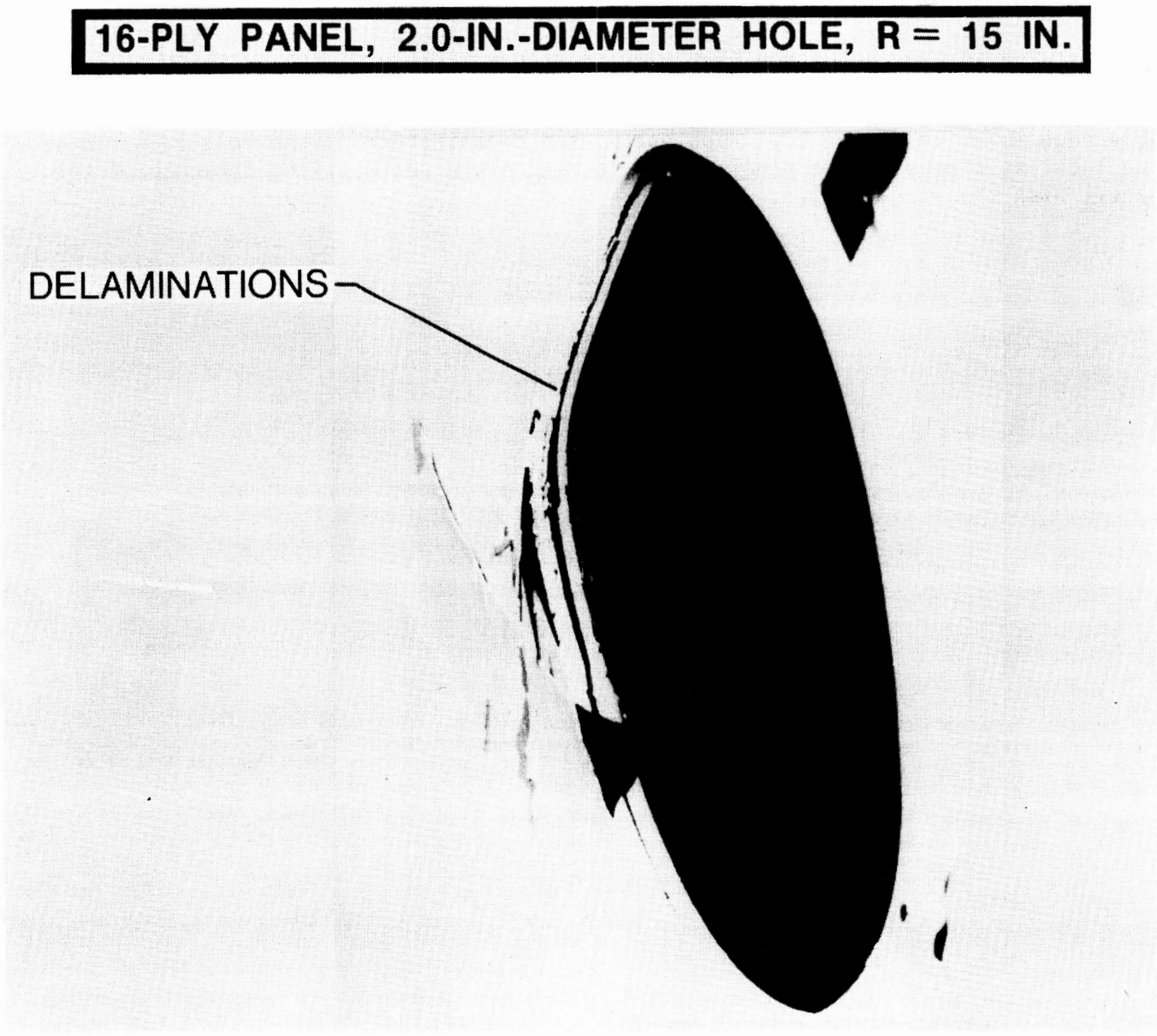

Figure 10

POSTBUCKLING ANALYSIS OF A CURVED GRAPHITE-EPOXY COMPRESSION PANEL WITH A HOLE

The STAGSC-1 nonlinear structural analysis code (ref. 3) was used in reference 5 to analyze the postbuckling response of the curved T300/5208 panel with a 2.0-inch-diameter hole described in Figure 9. The analytical results are compared with the test results in the upper left figure in Figure 11. The end shortening u (normalized by the panel length L) is shown as a function of the applied load P (normalized by the panel longitudinal modulus E and cross-sectional area A). Test and analysis compare reasonably well until the buckling load is approached. Near buckling the analysis predicts large symmetric local radial deflections w near the hole as indicated by the lower left contour and deformed shape plots for the load corresponding to point A on the upper left figure. An arc-length projection method (ref. 6) was used to continue the analysis past the limit point and onto the unstable postbuckling equilibrium path. After buckling the analysis predicts severe local bending and large nonsymmetric radial deflections near the hole as indicated by the lower center contour and deformed shape plots for the load corresponding to point B on the upper left figure. On the stable postbuckling equilibrium path, the analysis again predicts severe local bending and large nonsymmetric radial deflections as indicated by the lower right contour and deformed shape plots for the load corresponding to point C on the upper left figure. Apparently, the severe local bending near the hole causes sufficiently large surface rotations to exceed the capability of the moderate rotation formulation used in STAGSC-1. Also, this severe local bending apparently causes enough local transverse shearing deformations to delaminate the panel at the edge of the hole as shown in Figure 10. Once delamination occurs, the finite element model does not accurately represent the panel near the hole.

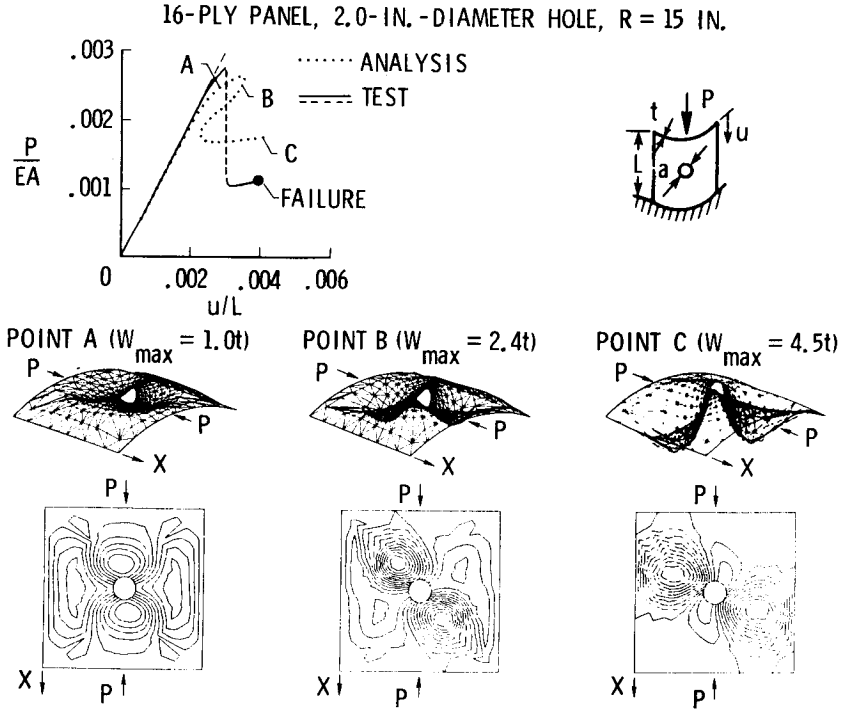

Figure 11

POSTBUCKLING RESPONSE OF CURVED GRAPHITE-EPOXY STIFFENED COMPRESSION PANELS

Curved graphite-epoxy stiffened panels were loaded to failure in compression to study their postbuckling behavior. The panels were made from T300/5208 graphite-epoxy tape and had an 85 inch radius. The panels had the same 16-ply-skin and stiffener designs as the flat panels described in Figure 5 and had a 4.0- or 7.0-inch stiffener spacing. The results of the tests of these panels are shown in Figure 12. End shortening results u (normalized by panel length L) are shown as a function of the applied load P (normalized by the panel longitudinal modulus E and cross-sectional area A). The results for the corresponding flat specimens from Figure 5 are shown for comparison. The square symbols represent the curved panel results and the circles represent the flat panels. The open symbols represent buckling and the filled symbols represent failure. As expected, buckling loads for both curved panels are higher than for the corresponding flat panels. However, the flat panel with 4.0-inch stiffener spacing failed at a higher load than the corresponding curved panel, and the curved panel with the 7.0-inch stiffener spacing failed at a higher load than the corresponding flat panel. Additional testing and analyses are currently being conducted to resolve this apparent anomaly.

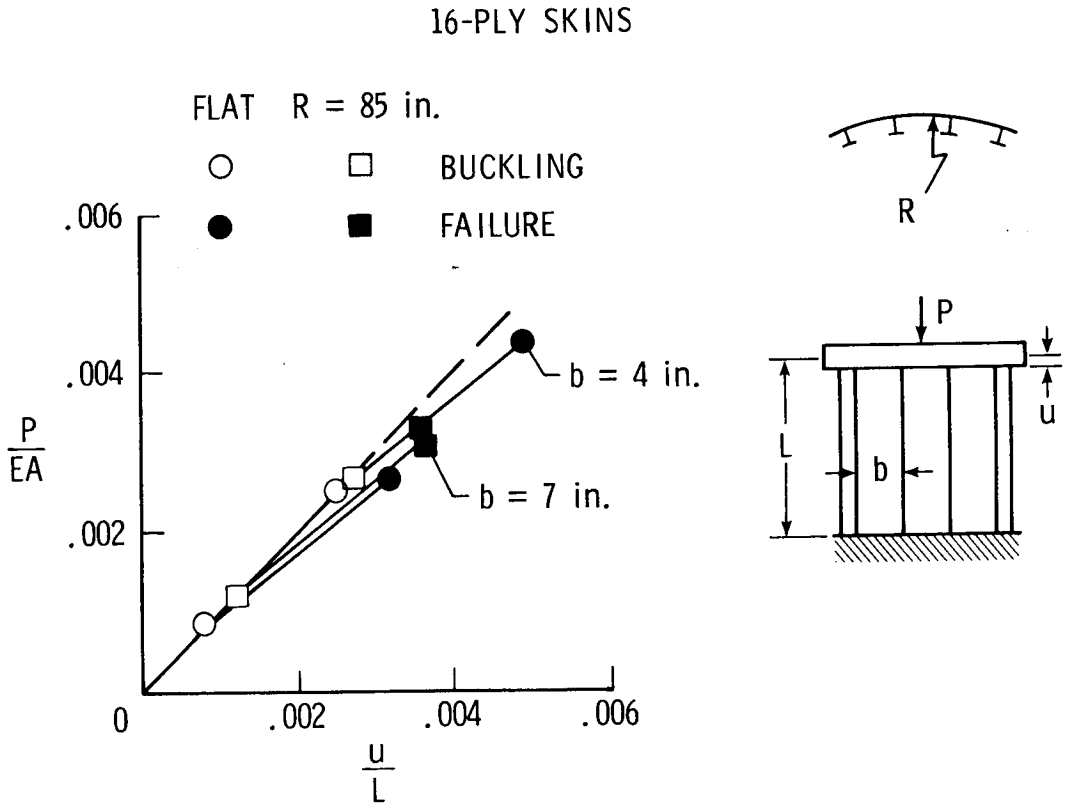

Figure 12

POSTBUCKLING RESPONSE OF UNSTIFFENED GRAPHITE-EPOXY SHEAR WEBS

Flat unstiffened shear webs were loaded to failure in shear to study their postbuckling behavior and failure characteristics. The results of this study of unstiffened shear webs are part of the research being conducted by the third author to fulfil the requirements for the degree of Master of Science from the School of Engineering and Applied Science of George Washington University. Unidirectional tapes of Hercules AS4 graphite fibers and 3502 epoxy resin (AS4/3502) were used to make 8-, 16-, and 24-ply webs with quasi-isotropic, orthotropic, and all-±45 stacking sequences. All of the webs had 12.0-inch by 12.0-inch test sections and were tested in a picture-frame shear fixture.

Membrane shear strain results are shown in figure 13. The applied load T is normalized by the applied load at buckling T_{cr} and the membrane shear strain γ is normalized by the membrane shear strain at buckling γ_{cr}. The open symbols indicate failure of the webs. The failure loads of the 8- and 16-ply webs were approximately 50 and 8 times the buckling load, respectively. The failure loads of the 24- and 32-ply webs were approximately 4.5 and 2.5 times the buckling load, respectively. There was a significant reduction in postbuckling stiffness as indicated by the change in slope of the postbuckling curves when the stacking sequence of the 8-ply webs was changed from a quasi-isotropic to an all-±45 laminate. The 16-ply quasi-isotropic and orthotropic webs had essentially the same postbuckling stiffness, but the all-±45 webs had a slightly lower postbuckling stiffness. The 24-ply webs had essentially the same postbuckling stiffness. Test results indicate that laminate stacking sequence and thickness can influence the postbuckling stiffness and strength of graphite-epoxy shear webs.

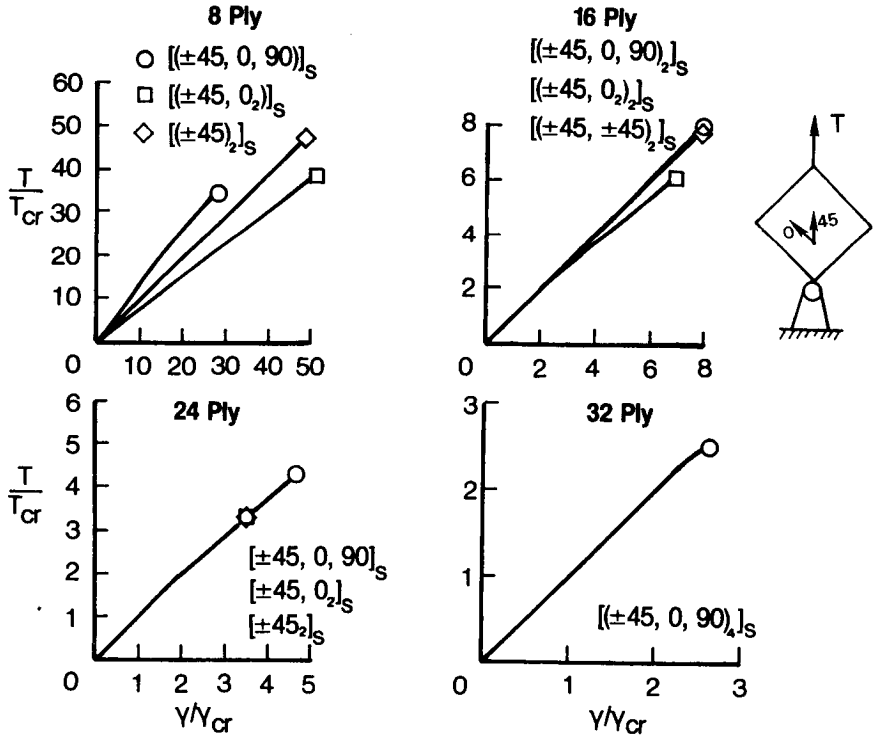

Figure 13

OUT-OF-PLANE DEFLECTIONS OF UNSTIFFENED SHEAR WEB

Out-of-plane deflections measured near a point of maximum buckling-mode amplitude are shown in Figure 14 for the 8-, 16-, and 24-ply webs described in Figure 13. The applied shear flow ($T/\sqrt{2}b$) is plotted on the vertical axis and the out-of-plane deflection w normalized by the web thickness is plotted on the horizontal axis. The symbols represent test data for the various laminates defined in the figure. The filled symbols indicate failure. The 8-ply webs had maximum out-of-plane deflections at failure of over five times the thickness. There was significant reduction in the maximum deflection when the thickness of the specimen was increased from 8 plies to 16 plies and a further reduction when the thickness was increased to 24 plies. The results shown in the figure indicate that a significant amount of bending can occur when a graphite-epoxy shear web is loaded into the postbuckling range and the bending stiffness is influenced by the thickness.

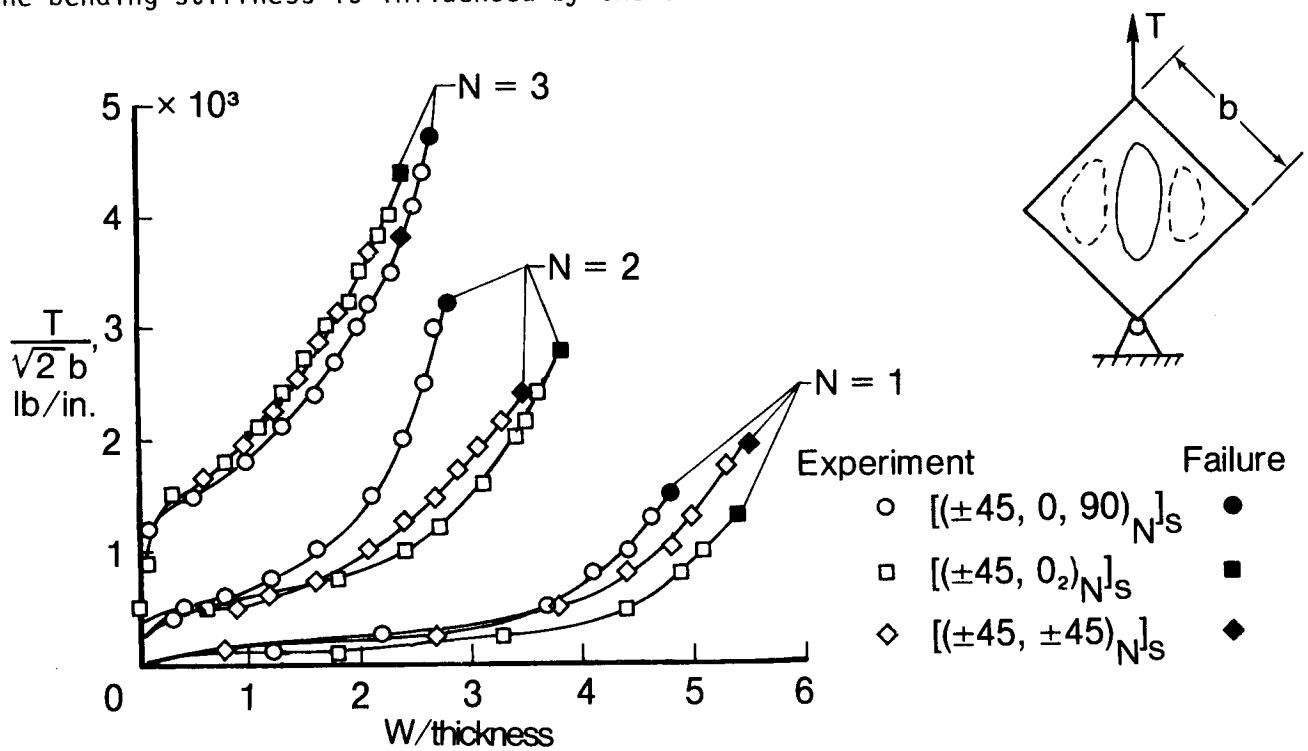

Figure 14

FAILURE CHARACTERISTICS OF AN 8-PLY SHEAR WEB

Some failure characteristics of an 8-ply shear web that was loaded into the postbuckling range are shown in Figure 15. The specimen was loaded well into the postbuckling range and then unloaded for inspection. The photograph on the left shows the moire-fringe pattern of the buckled web at its maximum load. The panel was cross sectioned so the interior could be examined. The center photographs show a cross section of the web. The photograph on the right shows the results of an ultrasonic C-scan inspection of the web.

The photograph of the moire-fringe pattern indicates that a high displacement gradient occurred near the center of the web prior to failure. The photograph of the ultrasonic C-scan indicates that a delamination had occurred in the web. The center photographs show a transverse crack in the laminate and a delamination between plies. Results for 8-ply shear webs indicate that delamination may be a failure mode limiting the postbuckling strength of a graphite-epoxy shear web.

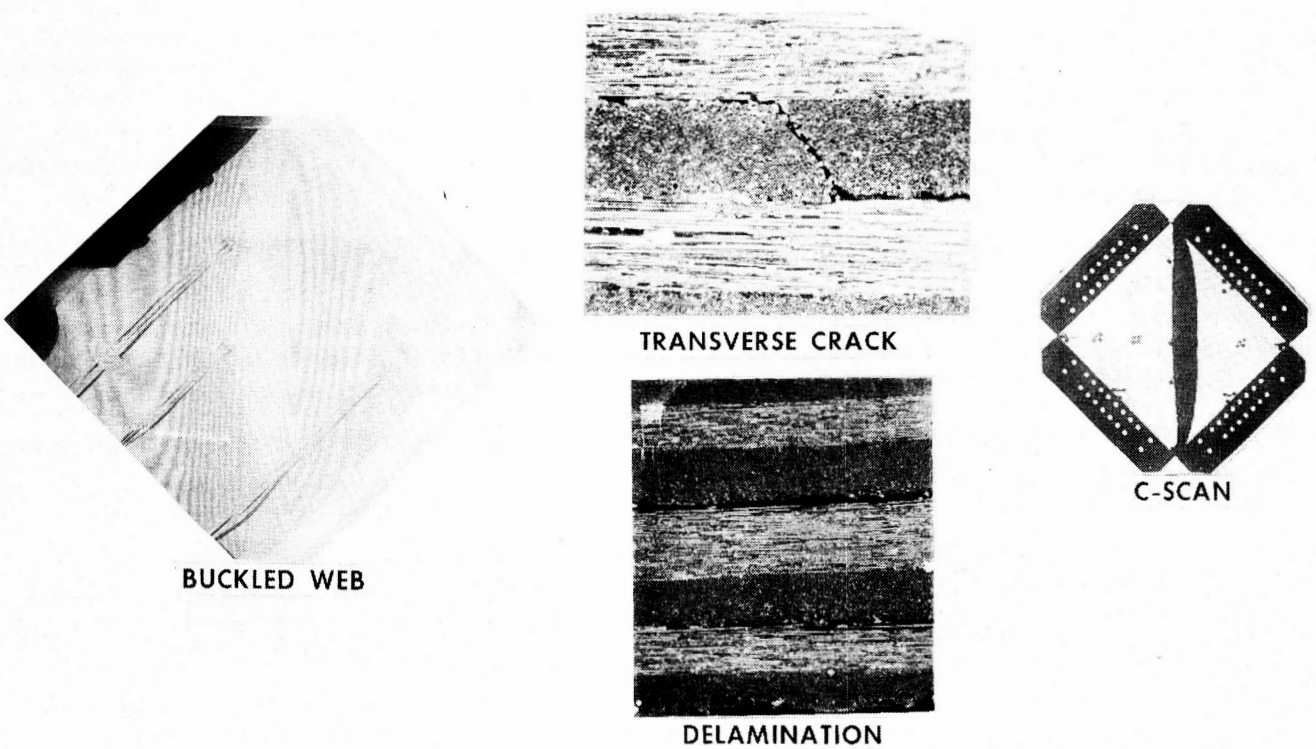

Figure 15

POSTBUCKLING BEHAVIOR OF STIFFENED GRAPHITE-EPOXY SHEAR WEBS

Flat stiffened graphite-epoxy shear webs were loaded to failure in shear to study their postbuckling behavior. Unidirectional tapes of Hercules AS4/3502 graphite-epoxy were used to make 19-, 25-, and 33-ply shear webs. All of the shear webs had 22.5-inch by 22.5-inch test sections. The 19-ply shear webs had a 4.5-inch stiffener spacing and the 25- and 33-ply webs had a 7.5-inch stiffener spacing. There was a common stiffener design for all of the webs that were tested. The stiffeners were attached to the skins with mechanical fasteners and/or bonding. A photograph of a 19-ply shear web is shown in the upper left of Figure 16.

Membrane shear strain results from the tests are summarized below in the lower left of Figure 16. The applied shear flow q is plotted as a function of membrane shear strain. Buckling is indicated by the open symbols and the filled symbols indicate failure. All of the shear webs exhibited some postbuckling capability. The 33-ply shear webs failed soon after buckling. The 19- and 25-ply shear webs had more postbuckling response after buckling. Test results for 25-ply shear webs indicate that specimens with mechanically fastened stiffeners did not exhibit significant improvements in postbuckling performance compared to the specimen with adhesively bonded stiffeners. An improved fastener concept did improve the postbuckling performance of 19-ply shear webs with mechanically fastened and adhesively bonded stiffeners. The photograph in the upper right of Figure 16 shows the typical failure mode for all of the shear webs. These specimens failed when the stiffeners separated from the skin along the skin-stiffener interface.

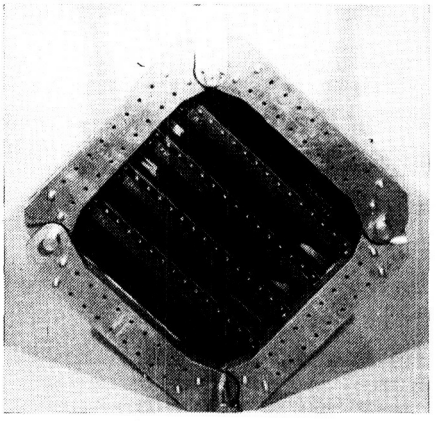

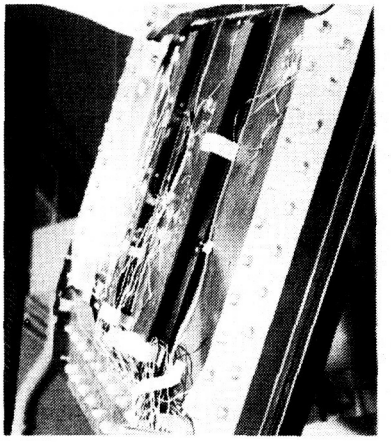

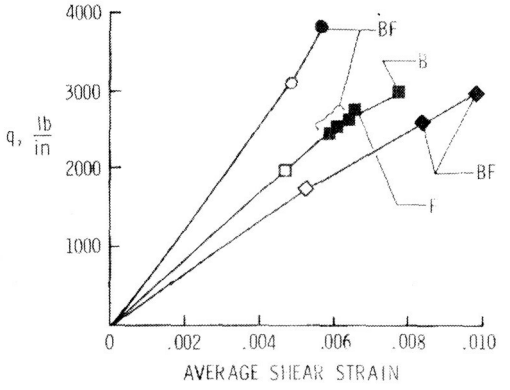

B - BONDED ONLY
F - MECHANICAL FASTENERS ONLY
BF - BONDED AND MECHANICAL FASTENERS

BUCKLING		FAILURE
○	$[(\pm 45, \mp 45)_2, 90_2, \bar{0}_S]_S$	●
□	$[(\pm 45, \mp 45)_2, 0_2, \overline{90}_S]_S$	■
◇	$[\pm 45, \mp 45, \pm 45, 90_2, \bar{0}_3]_S$	◆

Figure 16

POSTBUCKLING RESPONSE OF CURVED GRAPHITE-EPOXY STIFFENED PANELS LOADED IN SHEAR AND COMPRESSION

Curved AS4/3502 graphite-epoxy stiffened panels were loaded to failure in shear and combined shear and compression to study their postbuckling behavior. The panel designs were based on a minimum-weight buckled-skin design obtained from the POSTOP structural optimization code (ref. 7) and had both stiffeners and frames as indicated in Figure 17 below. The padded-skin stiffener attachment concept described in Figure 8 was used at each stiffener location and a failsafe strap was included under each frame and midway between each frame. The panels were 60 inches long, 42 inches wide and had a 143 inch radius. The panels were mounted in a D-box type fixture to provide a closed torque box suitable for shear loading and tested in the Lockheed-Georgia Company's multi-axis combined load test machine.

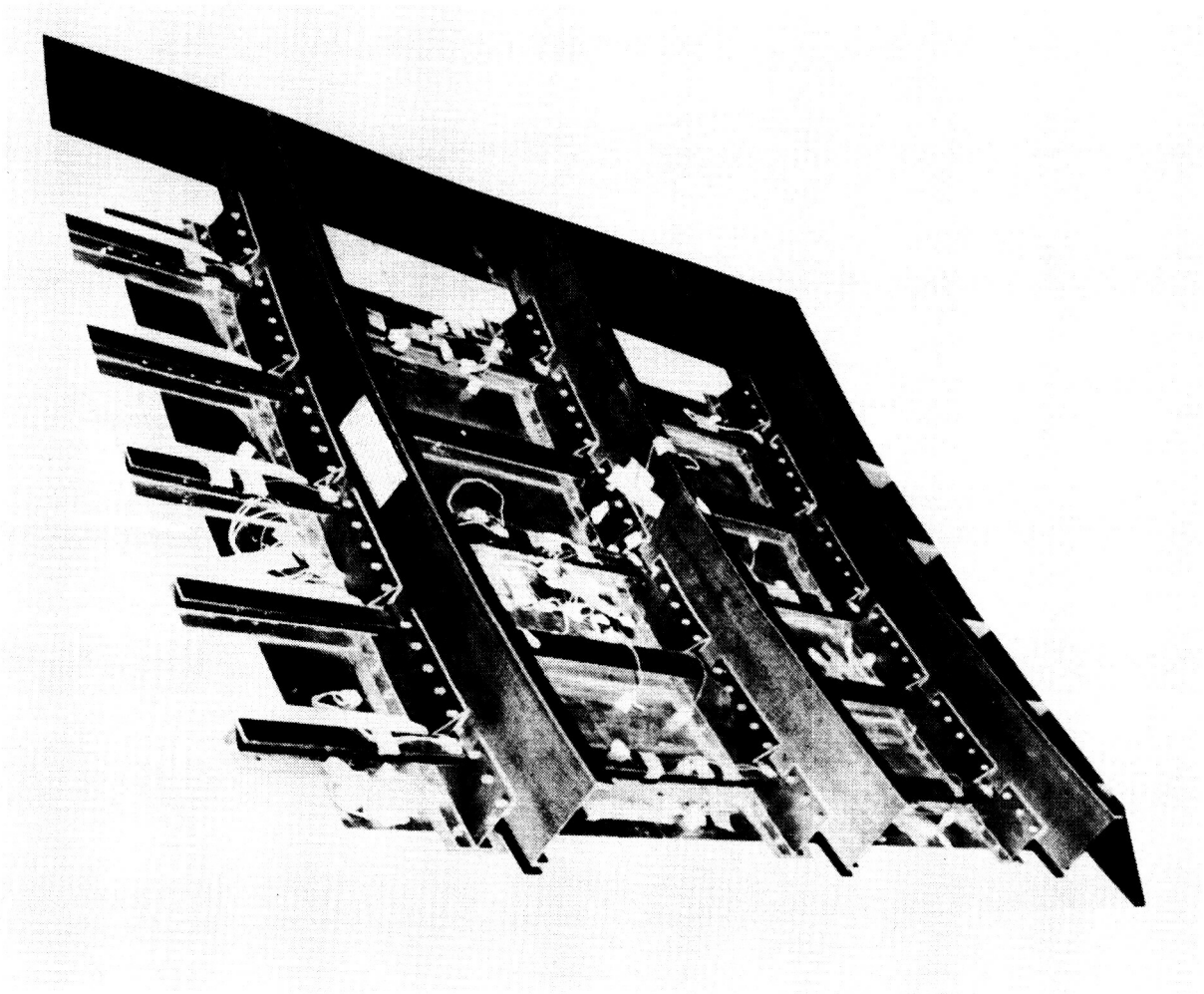

Figure 17

POSTBUCKLING RESPONSE OF CURVED GRAPHITE-EPOXY PANELS
LOADED IN SHEAR AND COMPRESSION

The results of the shear and combined shear and compression tests of the panels described in Figure 17 are shown in Figure 18. Three panels were tested to failure. The first panel was loaded in shear only, the second panel was loaded with approximately equal magnitudes of shear and compression stress resultants and the third panel was loaded with approximately three times as much compression as shear. The predicted buckling and failure interaction curves for shear N_{xy} and compression N_x loading are shown on the figure. The open circles on the figure represent the buckling data from the tests and the filled circles represent failure of the specimens.

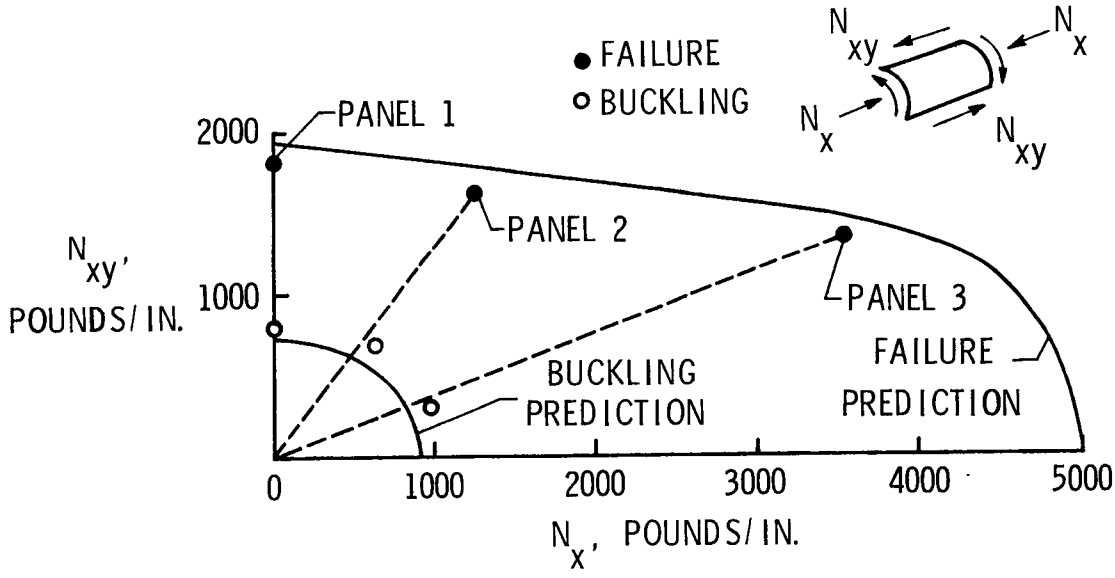

Figure 18

FAILURE MODES OF CURVED GRAPHITE-EPOXY PANELS
LOADED IN SHEAR AND COMPRESSION

A typical failed specimen that had been loaded in combined shear and compression is shown in Figure 19. The panel failed along a diagonal from frame to frame as shown in the left photograph. The stiffeners appear to have crippled where the diagonal failure intersected the stiffeners as shown in the magnified photograph of the stiffener on the right. No stiffener crippling was observed in the panel that was tested in shear only since no compression load was applied to the stiffeners of this panel. Some frame damage was observed after failure of the panel loaded in shear only; however the frame damage may have been caused by the test fixture.

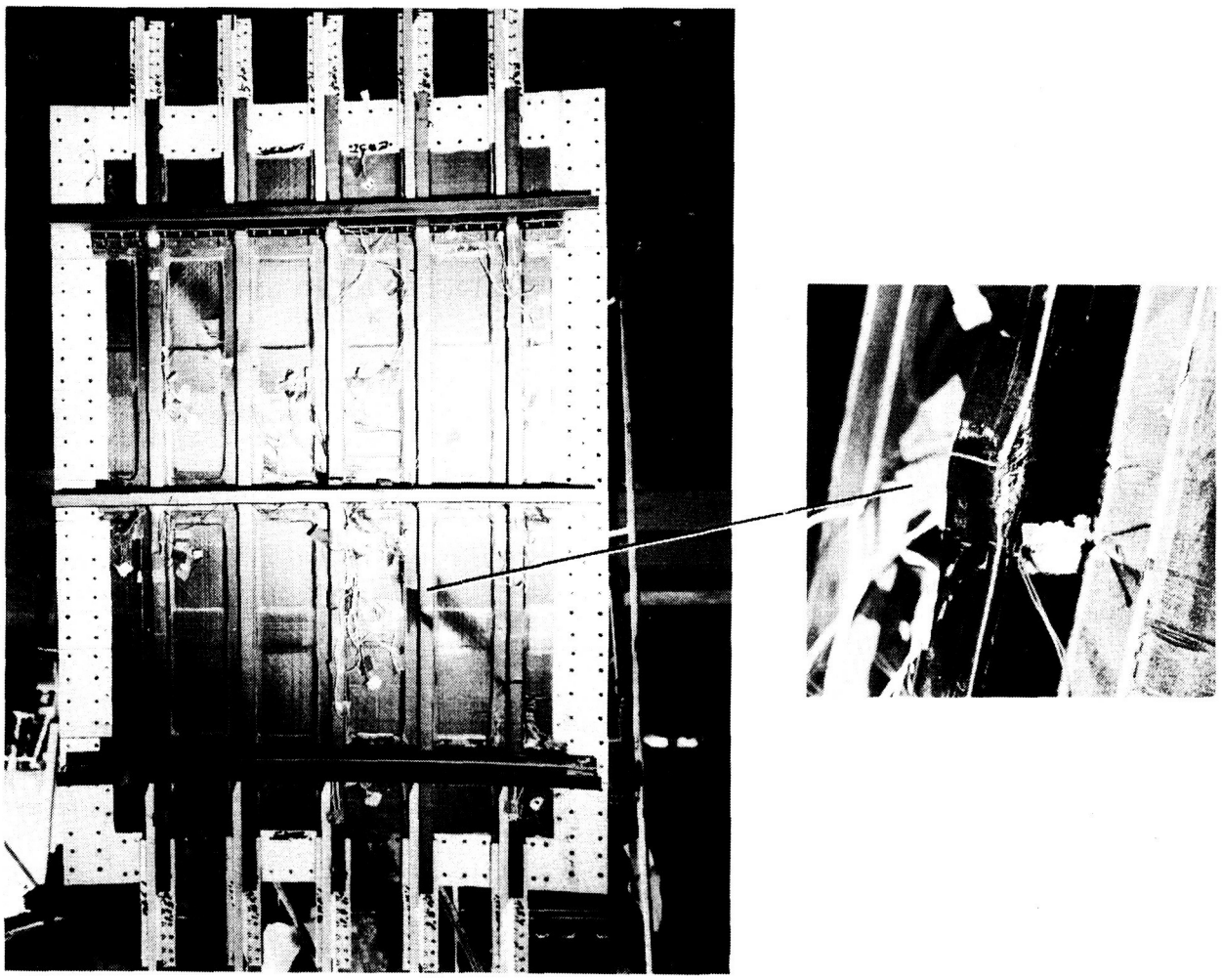

Figure 19

CONCLUDING REMARKS

- Graphite-epoxy structural components loaded in compression, shear and combined shear and compression can exhibit substantial postbuckling strength.
- Unstiffened laminates fail along buckling-mode nodal lines where interlaminar shear stresses are large.
- Holes and low-speed impact damage can degrade postbuckling strength if local strains are high enough to initiate and propagate damage.
- Postbuckling strength of stiffened panels can be limited by skin-stiffener separation.
- Increasing the skin thickness under a stiffener suppresses skin-stiffener separation.
- Stiffened panels can fail by stiffener crippling if skin-stiffener separation is suppressed.
- Damaged stiffeners can degrade postbuckling strength.
- Local delamination degrades postbuckling strength of curved panels with holes.
- Postbuckling response can be predicted analytically if local bending flexibility is adequately modeled.
- Large rotation and transverse shear deformation theories may be needed to accurately predict postbuckling behavior of components with severe local bending gradients.

REFERENCES

1. Starnes, James H., Jr.; and Rouse, Marshall: Postbuckling and Failure Characteristics of Selected Flat Rectangular Graphite-Epoxy Plates Loaded in Compression. Proceedings of the AIAA/ASME/ASCE/AHS 22nd Structures, Structural Dynamics and Materials Conference, Atlanta, GA, April 6-8, 1981. AIAA Paper No. 81-0543.

2. Starnes, James H., Jr.; Knight, Norman F., Jr.; and Rouse, Marshall: Postbuckling Behavior of Selected Flat Stiffened Graphite-Epoxy Panels Loaded in Compression. Proceedings of the AIAA/ASME/ASCE/AHS 23rd Structures, Structural Dynamics and Materials Conference, New Orleans, LA, May 10-12, 1982. AIAA Paper No. 82-0777.

3. Almroth, B. O.; Brogan, F. A.; and Stanley, G. M.: Structural Analysis of General Shells, Vol. II, User Instructions for STAGSC-1. Report No. LMSC-D633873, Lockheed Palo Alto Research Laboratory, Palo Alto, CA, December 1982.

4. Wang, J. T. S.; and Biggers, S. B.: Skin/Stiffener Interface Stresses in Composite Stiffened Panels. NASA CR-172261, January 1984.

5. Knight, Norman F., Jr.; and Starnes, James H., Jr.: Postbuckling Behavior of Axially Compressed Graphite-Epoxy Cylindrical Panels with Circular Holes. Collapse Analysis of Structures, Sobel, L. H. and Thomas, K., Eds., PVP Vol. 84, ASME, June 1984, pp. 153-167.

6. Riks, E.: The Application of Newton's Method to Problems of Elastic Stability. Journal of Applied Mechanics, Vol. 39, December 1972, pp. 1060-1066.

7. Dickson, J. N.; and Biggers, S. B.: POSTOP: Postbuckling Open-Stiffener Optimum Panels - Theory and Capability. NASA CR-172259, January 1984.